



## Photosynthetic performance of quinoa (*Chenopodium quinoa* Willd.) after exposure to a gradual drought stress followed by a recovery period

Arafet Manaa<sup>a,\*</sup>, Rahma Goussi<sup>a,b,c</sup>, Walid Derbali<sup>a,b</sup>, Simone Cantamessa<sup>c</sup>, Jemaa Essemine<sup>d</sup>, Roberto Barbato<sup>c</sup>

<sup>a</sup> Laboratory of Extremophile Plants, Centre of Biotechnology of Borj Cedria, B.P. 901, Hammam-Lif 2050, Tunisia

<sup>b</sup> Faculté des Sciences de Tunis, Université Tunis El Manar, 2092, Tunisie

<sup>c</sup> Dipartimento di Scienze e Innovazione Tecnologica, Università del Piemonte Orientale, viale Teresa Michel 11, 15121 Alessandria, Italy

<sup>d</sup> CAS Center for Excellence in Molecular Plant Sciences, Institute of Plant Physiology and Ecology, Shanghai Institutes for Biological Sciences, Chinese Academy of Sciences, Shanghai 200032, China

### ARTICLE INFO

#### Keywords:

Bioenergetics  
Chloroplast  
Drought  
Fluorescence  
Photosynthesis  
Quinoa  
Immunoblot analysis

### ABSTRACT

Drought is an abiotic scourge, one of the major environmental stress factors that adversely affect plant growth and photosynthesis machinery through a disruption of cell organelles, arrangement thylakoid membranes and the electron transport chain. Herein, we probed the effect of drought stress on photosynthetic performance of *Chenopodium quinoa* Willd. Beforehand, plants were subjected to water deficit (as 15% Field Capacity, FC) for one (D-1W) or two weeks (D-2W), and were then re-watered at 95% FC for 2 weeks. Light and electron microscopy analysis of leaves showed no apparent changes in mesophyll cell organization and chloroplast ultrastructure after one week of drought stress, while a swelling of thylakoids and starch accumulation were observed after the prolonged drought (D-2W). The latter induced a decrease in both PSI and PSII quantum yields which was accompanied by an increase in  $F_0$  (minimum fluorescence) and a decline in  $F_m$  (maximum fluorescence). Drought stress influenced the fluorescence transients, where the major changes at the OJIP prompt FI level were detected in the OJ and IP phases. Prolonged drought induced a decrease in chl *a* fluorescence at IP phase which was readjusted and established back after re-watering and even more an increase was observed after 2 weeks of recovery. The maximum quantum yield of primary photochemistry ( $\phi_{P_0}$ ) was unaffected by the different drought stress regimes. Drought induced an increase in the ABS/RC and  $DI_0$ /RC ratios which was concurrent to a stable  $\phi_{P_0}$  (maximum quantum yield of PSII primary photochemistry). A substantial decrease in  $PI_{(ABS)}$  was detected especially, during severe drought stress (D-2W) suggesting a drop in the PSII efficiency and the level of electron transport through the plastoquinone pool (PQ pool) towards oxidized PSI RCs ( $P_700^+$ ). The immunoblot analysis of the main PSII proteins revealed considerable changes in the D1, D2, CP47, OEC, PsbQ and LHCII proteins under drought. These changes depend on the stress duration and recovery period. The main message of this investigation is the elevated recovery capacities of PSII and PSI photochemical activities after re-watering.

### 1. Introduction

Drought is considered as one of the most important environmental stresses, particularly in arid and semi-arid agro-ecosystems where plants are frequently exposed to repeated and harsh water deficit periods, affecting plant growth and development, and subsequently the agricultural crop yields [1–3]. Drought effects on the physiological and biochemical processes are nowadays well understood; the primary effect of water deficit is the stomatal closure which allows plants to limit

transpiration [4]. In addition, a decrease in the relative water content (RWC) and leaf water potential [5] were also recorded in case of water shortage. Photosynthesis is one of the most sensitive processes to drought [6] which leads to the decrease of internal  $CO_2$  concentration by limiting its diffusion through the stomata and the mesophyll cells [7–9], the decrease of stomatal conductance and the alterations of carbon assimilation [1]. Drought stress induces several others changes at the cellular level such as loss of membrane integrity and lipid peroxidation generated by reactive oxygen species (ROS) production and

\* Corresponding author.

E-mail address: [arafet.manaa@cbbc.rnrt.tn](mailto:arafet.manaa@cbbc.rnrt.tn) (A. Manaa).

<https://doi.org/10.1016/j.bbabio.2021.148383>

Received 23 June 2020; Received in revised form 11 January 2021; Accepted 21 January 2021

Available online 26 January 2021

0005-2728/Published by Elsevier B.V. This article is made available under the Elsevier license (<http://www.elsevier.com/open-access/userlicense/1.0/>).

accumulation [10] as a common sign of oxidative stress caused also by other abiotic stresses [11–13]. In contrast, drought resistant plants have developed various adaptive strategies to cope with water deficit [11,14]. These adaptive mechanisms can be summarized in: (i) morphological changes such as reduced leaf area and stomatal conductance allowing the reduction in water loss and developing of profound root systems reaching deeper water sources [15]; (ii) osmotic adjustment through the synthesis of compatibles solutes and osmolytes such as proline, polyamines, and glutathione [16]; (iii) increase in the scavenging capacity for ROS via increase in antioxidant enzymes like SOD, POD, CAT, APX, GR and MDHR [11,12]; (iv) induction of ABA accumulation and increased expression in ABA biosynthesis genes mediating plant water balance and osmotic stress tolerance [17,18].

Particularly, there are some crops mostly well-adapted to these harsh climatic conditions such as water deficit, which includes quinoa [19]. Quinoa (*Chenopodium quinoa* Willd.) is a facultative halophyte which belongs to the C<sub>3</sub> plants, and whose genome ( $2n = 4x = 36$ ) has been recently sequenced [20]. It is known as an important food source in the Andean region for thousands of years [21–23], and emerges as a good food candidate due to its exceptional nutritive value, the high number of genotypes, and diverse adaptability to various abiotic stresses (USGS, United States Geological Survey 2010) such as salinity [22,24–26], drought [21,27–29], frost [30,31], as well as an ability to grow on marginal soils [32,33]. Quinoa is considered as staple food in many countries under the global climate changes which affect the growth conditions of crops and influence food production and distribution, as well as associated consequences for human food and nutrition security [34,35]. Quinoa is traditionally called the mother of grains, owing the potential to provide a highly nutritious food source because its seeds contain an excellent balance of essential amino acids, fibers, lipids, carbohydrates, vitamins, and minerals [36–38]. Due to these properties, quinoa has gained global attention of the scientific community in the last decade when 2013 was declared as the “International Year of Quinoa” by Food and Agriculture Organization (FAO) to attract attention to this alternative crop that can cope with the increasing scarcity of fresh water resources and an increasing soil salinization [39].

Quinoa responses to drought stress have been well documented and their tolerance mechanisms to stress were also reported, most of which are common to most of higher plants as highlighted above. Nevertheless, some specific mechanisms are not yet completely understood for quinoa plant, especially, the photosynthesis which constitutes the primary target influenced by water deficit. In this way, different methods and biophysical tools (PAM analysis, chlorophyll *a* (Chl *a*) fluorescence, Fast Fluorescence decay, OJIP test, etc.) were previously used to demonstrate their applicability to research into the response of the photosynthetic apparatus and plant tolerance to unfavorable environmental conditions [40–42]. However, there is a limited amount of other substantiation regarding the effect of drought on halophyte photosynthetic apparatus and so further research is necessary on this topic. Earlier reports demonstrated that the stress release induced a restoration of plant growth as previously described in *Eugenia myrtifolia* [43], *Solanum lycopersicum* [44] and in two forage species, *Medicago truncatula* and *Sulla carnosa* [45]. Our hypothesis is that this recovery capacity could be tightly associated with the ability of preserving functional photochemical activity. The main objective of the present work is to analyze the effect of drought stress on photosynthetic apparatus (PA) based on different anatomical, biochemical and biophysical approaches. We also want to estimate the recovery capacity of photosynthetic performance after re-watering using chloroplast ultrastructure, Chl fluorescence and immunoblot analysis of thylakoidal proteins. Such study will provide valuable and reliable insights about the photosynthetic process involved in stress tolerance mechanism of quinoa and will generate additional knowledge about the resistance mechanisms in halophyte and define other physiological and biophysical markers for stress tolerance.

## 2. Material and methods

### 2.1. Plant growth conditions

In this study we used *Chenopodium quinoa* (Var. Red Faro) originally collected from southern Chile and provided by the United States Department of Agriculture (USDA). Seeds were surface sterilized for 5 min by soaking in a solution of sodium hypochlorite 20% (v/v), then rinsed generously (up to 5 times) with distilled water. Subsequently, quinoa seeds were sown in 0.6-L plastic pots (at a rate of 4 seeds per pot) filled with limono-sandy soil containing: (meq 100 g<sup>-1</sup> of dry soil) 0.25 Na<sup>+</sup>, 0.95 K<sup>+</sup>, 0.65 Ca<sup>2+</sup>, and 0.05 Cl<sup>-</sup>; and (g kg<sup>-1</sup> dry soil) 0.24 P<sub>2</sub>O<sub>5</sub> and 0.45 total nitrogen (N). The pH and the electrical conductivity of the aqueous extract (1/10) were 6.68 and 0.05 dSm<sup>-1</sup>, respectively. The soil field capacity (FC) was determined according to [46] which was around 11%. Seedlings were grown in a climate-controlled greenhouse with temperature of 25/18 °C and relative humidity of 60/70% day/night, respectively. Seedlings were irrigated with distilled water for the first week of germination and then with the full-strength nutrient [47] solution containing: 3.5 mM Ca(NO<sub>3</sub>)<sub>2</sub>, 3.0 mM KNO<sub>3</sub>, 1.5 mM MgSO<sub>4</sub>, 1.6 mM KH<sub>2</sub>PO<sub>4</sub>, 0.6 mM K<sub>2</sub>HPO<sub>4</sub>, 3 μM Fe–K-EDTA, 0.05 μM H<sub>3</sub>BO<sub>3</sub>, 0.5 μM MnSO<sub>4</sub>, 0.04 μM CuSO<sub>4</sub>, 0.05 μM ZnSO<sub>4</sub>, and 0.02 μM (NH<sub>4</sub>)<sub>6</sub>Mo<sub>7</sub>O<sub>24</sub>. Twenty day-old seedlings were subjected to a phase of acclimation (7 days) during which soil was maintained at 95% field capacity (FC). After one week of acclimation, plants were subjected to different water treatments as schematically depicted in Fig. 1.

Ctrl: plants were irrigated with tap water at 95% FC (well-irrigated treatment).

D-1W: water-deficit stressed plants irrigated with tap water at 15% FC, for 1 week.

D-2W: water-deficit stressed plants irrigated with tap water at 15% FC, for 2 weeks.

Rec–D1: Drought-stressed plants (D-1W) were re-watered at 95% FC.

Rec–D2: Drought-stressed plants (D-2W) were re-watered at 95% FC.

The period of recovery was maintained for 2 weeks for each drought treatment. Irrigation was performed every 2 days (regular weighing) to restore the soil moisture at 95 or 15% FC. During the drought period 2 g of slow release Osmocote (10 N:11P:18 K) was added to the soil mixture in order to maintain the same quantity of nutrients received by all treated or untreated plants.

### 2.2. Leaf osmotic potential

The leaf osmotic potential ( $\Psi_s$ ) was probed as previously described in [48]. Quinoa leaves were quickly collected, cut into small segments, then placed in Eppendorf tubes perforated with four small holes and immediately frozen in liquid nitrogen. After being encased individually in a second intact Eppendorf tube, they were then kept for about 20 min at room temperature for thawing before being pressed. The collected tissue sap was analyzed for ( $\psi_s$ ) estimation. Osmolarity (C) was assessed with a vapour pressure osmometer (Wescor 5500; Inc., UT, USA) and converted from mosmoles kg<sup>-1</sup> to MPa according to the Van't Hoff equation:

$\Psi_s = -RTM$ , where R represents the universal gas constant, T stands for the temperature (K) and M is the osmolality.

### 2.3. Plant growth and chlorophyll content

In order to study the effect of drought stress and its recovery process on plant growth, different harvests were performed (Fig. 1). During each harvest, plant growth was determined by measuring the plant fresh weight (FW) and dry weight (DW) after desiccation at 70 °C for 3 days. For pigments analysis, quinoa fresh leaves (approximately 2.5 cm<sup>2</sup>) collected from leaf lamina were thereafter ground using pestle and

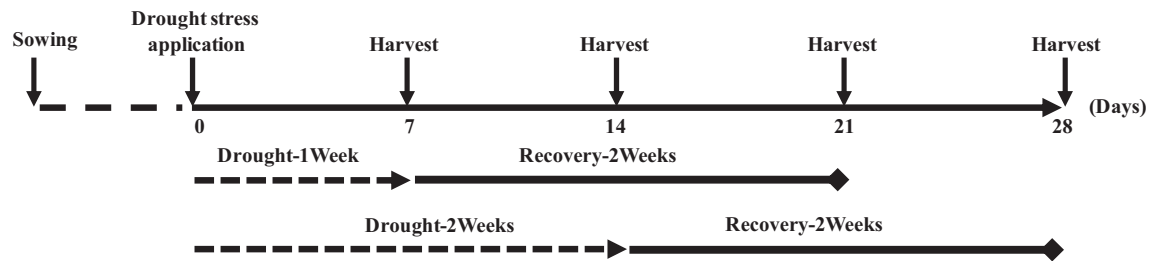


**Fig. 1.** Schematic diagram showing the experimental procedure for cultivating quinoa in presence and absence of drought stress. Drought stress was applied for either one week (D-1W) or two weeks (D-2W), each drought treatment was followed by a recovery period of two weeks. Four harvests were performed after 7, 14, 21 and 28 days after the beginning of stress application.

mortar, then extracted in a total volume of 5 ml of acetone 80% (v/v). The Chl extract was centrifuged at 3.000 g for 5 min. The supernatants were collected and Chl a, Chl b, total Chl content and Chl a/b ratio were calculated following the equations of [49]:

$$\text{Chl}_a = 12.25A_{663} - 2.79A_{645}$$

$$\text{Chl}_b = 21.50A_{645} - 5.10A_{663}$$

$$\text{Chl}_{tot} = 7.15A_{663} + 18.71A_{645}$$

The  $C_b = 21.50A_{645} - 5.10A_{663}$  Chl content was measured after each harvest and expressed as  $\mu\text{g} \cdot \text{g}^{-1} \text{FW}$ .

#### 2.4. Light and transmission electron microscopy

The structure and the ultrastructure of chloroplasts were analyzed independently in control and all drought-treated samples, using both light and transmission electron microscopy as previously described in [50]. Briefly, leaf segments of approximately 0.5 mm in length were fixed with 1% glutaraldehyde in 0.1 M sodium cacodylate buffer (pH 7.4) for 1 h at room temperature. The samples were then washed in phosphate-buffered saline and post-fixed in 1% (w/v)  $\text{OsO}_4$  similarly buffered for 2 h at 4 °C. The specimens were dehydrated in a graded ethanol series and propylene oxide, infiltrated and embedded in Epon 812 resin [51].

Semi-thin sections of the samples were stained with toluidine blue and studied under a Zeiss Axiophot light microscope connected to a digital camera (Axiocam, Zeiss) with image analysis software. Additionally, ultrathin sections were cut from the same samples and were collected on 150-mesh copper grids, and double stained with 2% (w/v) uranyl acetate for 40 min and with 3% (w/v) lead citrate for 3 min [52] and then photographed using a Transmission Electron Microscope (TEM, Philips EM 201) at 75 kV.

#### 2.5. Measurement of fast fluorescence induction kinetics (OJIP-curves) and PAM saturating pulse method analysis

The Chl a fluorescence induction (FI) kinetics was measured at room temperature using a Plant Efficiency Analyzer (Handy PEA, Hansatech Ltd., Norfolk, England) as previously described in [50]. Notably, leaves were dark adapted for 30 min before the determination of the minimum fluorescence ( $F_0$ ) when all PSII RCs are open and maximum fluorescence ( $F_m$ ) when all PSII RCs are closed. Light intensity reaching the leaf was  $3000 \mu\text{mol} \cdot \text{m}^{-2} \cdot \text{s}^{-1}$  which was sufficient to generate maximum fluorescence for control and all drought treatments. Chl a fluorescence transient was measured as previously reported in [53,54]. The OJIP-curves were normalized at both  $F_0$  and  $F_m$  and a series of parameters ( $V_{OP}$ ,  $V_{OK}$  and  $V_{OJ}$ ) were calculated according to [53–55]. The differences among relative variable fluorescence curves ( $\Delta V_{OK}$  and  $\Delta V_{OJ}$ ) between untreated (Ctrl) and drought-treated plants were defined as the so called L- and K-bands, respectively.

The so-called JIP-test was also performed using Biolyzer v.3.0.6

software (Chl fluorescence analyzing program by Laboratory of

**Table 1**

Definitions and explanations of selected JIP-test parameters derived from the chlorophyll a fluorescence induction curve.

Fluorescence parameters	Description
$F_0 \equiv F_{20\mu\text{s}}$	Minimal fluorescence when all the reaction centers are open
$F_K \equiv F_{300\mu\text{s}}$	Fluorescence intensity at 300 $\mu\text{s}$
$F_J \equiv F_{2\text{ms}}$	Fluorescence intensity at the J-step (2 ms) of OJIP
$F_I \equiv F_{30\text{ms}}$	Fluorescence intensity at the I-step (30 ms) of OJIP
$F_m(\equiv F_P)$	Maximal recorded fluorescence intensity, at the peak P of OJIP when all PSII reaction centers are closed
$F_v = (F_m - F_0)$	Variable chlorophyll fluorescence
$t_{Fm}$	Time to reach the maximal fluorescence intensity $F_m$
$V_t = (F_t - F_0)/(F_m - F_0)$	Relative variable fluorescence at time t
$V_I = (F_I - F_0)/(F_m - F_0)$	Relative variable fluorescence at the I-step
$V_J = (F_J - F_0)/(F_m - F_0)$	Relative variable fluorescence at the J-step
$M_0 = (\Delta V/\Delta t)_0 = 4(F_{300\mu\text{s}} - F_0)/(F_m - F_0)$	Approximated initial slope (in $\text{ms}^{-1}$ ) of induction curve $V_t$ (for $F_0 = F_{20\mu\text{s}}$ )
Area	Integrated area between the induction curve and the line $F=F_m$ relates to the pool size of PSII electron transport acceptors
$S_M = \text{Area}/F_v$	Normalized area (reflecting multiple turnover $Q_A$ reduction events and representing the number of electrons that have to flow through the electron transport chain in order to reach $F_m$ )
$N = S_M M_0 (1/V_J)$	Number of $Q_A$ redox turn over until $F_m$ is reached
$\text{ABS}/\text{RC} = M_0 (1/V_J) (1/\varphi_{P_0})$	Absorption flux (for PSII antenna chlorophylls) per reaction center (RC)
$\text{TR}_O/\text{RC} = M_0 (1/V_J)$	Trapped energy flux (leading to $Q_A$ reduction) per reaction center RC
$\text{ET}_O/\text{RC} = M_0 (1/V_J) \psi_0$	Electron transport flux (further than $Q_A$ ) per PSII RC(at t = 0)
$\text{DI}_O/\text{RC} = (\text{ABS}/\text{RC}) - (\text{TR}_O/\text{RC})$	Dissipated energy flux per reaction center RC (at t = 0)
$\varphi_{P_0} = \text{TR}_O/\text{ABS} = F_v/f_m = [1 - (F_0/f_m)]$	Maximum quantum yield of primary photochemistry (at t = 0)
$\psi_0 = \text{ET}_O/\text{TR}_O = (1 - V_J)$	Probability that a trapped exciton moves an electron further than $Q_A$
$\varphi_{E_0} = \text{ET}_O/\text{ABS} = [1 - (F_0/f_m)] \psi_0$	Probability that an absorbed photon moves an electron further than $Q_A$
$\text{ABS}/\text{CSm} = F_m$ (at t = $t_{Fm}$ )	Absorption flux per excited cross section, approximated by $F_m$
$\text{TR}_O/\text{CSm} = \varphi_{P_0} (\text{ABS}/\text{CSm})$ (at t = $t_{Fm}$ )	Trapped energy flux per excited cross section, approximated by $F_m$
$\text{DI}_O/\text{CSm} = (\text{ABS}/\text{CSm}) - (\text{TR}_O/\text{CSm})$ (at t = $t_{Fm}$ )	Dissipated energy flux per excited cross section, approximated by $F_m$
$\text{ET}_O/\text{CSm} = \varphi_{E_0} (\text{ABS}/\text{CSm})$ (at t = $t_{Fm}$ )	Electron transport flux per excited cross section, approximated by $F_m$
$\text{RC}/\text{CSm} = \psi_0 (V_J/M_0)(\text{ABS}/\text{CSm})$	Density of reaction centers per excited cross-section (at t = $t_{Fm}$ )
$\text{RC}/\text{ABS} = [(F_{2\text{ms}} - F_0)/4(F_{300\mu\text{s}} - F_0)](F_v/f_m)$	Density of reaction centers per chlorophyll
$\text{PI}_{(\text{ABS})} = (\text{RC}/\text{ABS}) (\varphi_{P_0}/(1 - \varphi_{P_0})) - (\psi_0/(1 - \psi_0))$	Performance index on absorption basis
$\text{PI}_{(\text{CSm})} = (\text{RC}/\text{CSm}) (\varphi_{P_0}/(1 - \varphi_{P_0})) - (\psi_0/(1 - \psi_0))$	Performance index on cross section basis

Bioenergetics, University of Geneva, Switzerland) [56]. Detailed insights and explanation about JIP-test parameters are available in Table 1. Data were also visualized by generating spider plots of bioenergetic fluxes.

The quantum yields and energy conversion in both photosystems (PSI and PSII) were evaluated simultaneously using saturating pulse analysis method of Dual-PAM 100 system (Heinz Walz GmbH, Germany) with Chl fluorescence absorption analyzer equipped with a P700 dual wavelength emitter-detector at 830 and 875 nm [57,58]. Plants were dark-adapted for 30 min before each measurement. A saturating pulse of white actinic light, AL (SP, width = 300 ms and intensity 10,000  $\mu\text{mol photons m}^{-2} \text{s}^{-1}$ ) was applied to determine the maximum fluorescence in the dark-adapted state ( $F_m$ ) and the absorbance parameters. A rapid light curve was triggered with increasing PAR (photosynthetically active radiation) levels from 20 to 1966  $\mu\text{mol photons m}^{-2} \text{s}^{-1}$  with 1 min exposure for each light step (level). The Chl fluorescence quenching parameters were calculated as described in [59]. All cited parameters in this section were measured independently at each harvest point or time (Fig. 1).

## 2.6. Thylakoid proteins extraction and immunoblot analysis

Thylakoid isolation, sodium dodecyl sulfate polyacrylamide gel electrophoresis (SDS-PAGE) and immunoblot gel membrane were performed as previously described in [60]. Leaves were ground to a fine powder and homogenized in an ice-cold solution buffer containing 50 mM Hepes (pH 7.2), 5 mM  $\text{MgCl}_2$ , 10 mM NaCl, 500 mM sucrose and 0.1% bovine serum albumine (BSA) [61]. The homogenate was filtered through four layers of cheese cloth and the filtrate was centrifuged at 5000 g for 10 min at 4 °C. The pellets were washed twice with the same isolation buffer without sucrose and finally suspended in 50 mM Hepes-NaOH pH 7.2, 5 mM  $\text{MgCl}_2$ , 10 mM NaCl containing 0.1 M sucrose. The Chl content was determined by measuring the optical density (OD) of the samples using spectrophotometer as described in [62].

SDS-PAGE and immunoblotting were performed as previously described in [61]. Thylakoid samples were subjected to SDS-PAGE where each gel lane was loaded with 4  $\mu\text{g}$  of protein extract; the separated proteins were transferred onto nitrocellulose membranes. Subsequently, the latter was then blocked for 1 h in 10% skimmed milk and probed with the specific primary antibodies. Immunodetection was performed by incubation with alkaline phosphatase conjugate method using goat-antirabbit secondary antibody and 5-bromo-4-chloro-3-indolyl phosphate/nitro blue tetrazolium (NBT) as chromogenic substrates. Proteins were probed using antibodies raised against the following proteins: D1(1:400), D2 (1:400), CP47 (1:800), LHClI (1:5000), PsbQ (1:400) and PsbO (1:800) according to [61]. The amount of each of these proteins was determined by quantifying the intensities of immuno-reactions using *ImageJ* software.

## 2.7. Data analysis

Results are presented as means more or less ( $\pm$ ) standard error of six replicates for plant growth, leaf water potential and pigment analysis, but uniquely three replicates for the fluorescence measurements were performed on three different leaves, during each experiment, which was repeated twice (18 replicates in total). Statistical differences between measurements in different treatments were analyzed using one-way ANOVA and Duncan's multiple range tests where  $P < 0.05$  was considered statistically significant. Statistical analyses were performed using a professional software OriginPro (version 9.0 SR2; Northampton MA01060 USA).

## 3. Results

### 3.1. Plant growth capacity and Chl content

The phenotype and morphological aspect of quinoa plants cultivated under different water deficit regimes were displayed in Fig. 2. Compared to control, plant submitted to drought stress for 1 week (D-1W) showed no apparent change in plant phenotype or canopy morphology. However, a considerable reduction in the plant growth was observed following 2 weeks exposure to drought (D-2W) without appearance of any stress-induced damages including leaf rolling, chlorosis, and necrosis. After 2 weeks of rehydration, a nearly complete plant growth restoration was observed only for plants that have been drought-stressed for 1 week (Rec-D1). Plant growth was also evaluated by the percentage (%) of DW reduction relative to the Ctrl (Figs. 2 and 3A). Our results show a significant decrease in the entire plant DW about 16% and 52% after exposure of quinoa plants to D-1W and D-2W, respectively. The decrease in DW was attenuated after re-watering (Figs. 2 and 3A). This alleviation in DW was about 4% and 39% for Rec-D1 and Rec-D2, respectively (Figs. 2 and 3A).

Drought treatment induced also substantial changes in the Chl content irrespective of water regime (Table 2). Accordingly, drought stress for one week (D-1W) had no significant effect on either Chl *a*, Chl *b* or total Chl content, while a significant decrease ranging from 31 to 32%, relative to (Ctrl), was observed for all Chl pigments measured after 2 weeks of water deficit (D-2W). After a recovery period of 2 weeks (Rec-D2), the decrease in Chl content was relieved (Table 2). Hence, this decline in Chl content was merely about 19.5%, 24.3% and 20%, relative to the Ctrl, for Chl *a*, Chl *b* and total Chl content, respectively (Table 2). Regarding the Chl *a/b* ratio, a decrease by about 13% was recorded uniquely for (D-1W) and (Rec-D1) treatments if compared to control without stress (Table 2).

### 3.2. Leaf osmotic potential

Leaf osmotic potential significantly decreased in quinoa plant subjected to water-deficit stress with a drastic effect obviously observed in drought-stressed plant for 2 weeks (D-2W) (Fig. 3B). This decrease was about 25% and 45% for drought-stressed plants for 1 week (D-1W) and 2 weeks (D-2W), respectively (Fig. 3B). After 2 weeks of rehydration of drought-stressed-plant, a restoration in this physiological parameter (osmotic potential) to a similar level recorded for control plants was observed for both drought recovery regimes (Rec-D1 and Rec-D2; Fig. 3B).

### 3.3. Changes in the chloroplast ultrastructure

Changes in the chloroplast structure were investigated using a light microscope and TEM (Fig. 4A, B). It is worthy to note that only drought stress treatment of 2 weeks (D-2W) affects substantially the shape of leaf mesophyll cells (MC). The latter takes an irregular shape and the epidermal cells were thinner if compared to the control without stress (Fig. 4A). Following both recovery regimes (Rec-D1 and Rec-D2), leaf mesophyll shape was similar to that observed for well-irrigated plants (Ctrl). The TEM observation of control leaves showed a typical and well differentiated chloroplast containing well compartmentalized grana stacks and well-developed stroma lamellae paralleled the chloroplasts long axes (Fig. 4B). We noticed the appearance of few plastoglobuli (PL) in the stroma lamellae (SL) in the control samples chloroplasts. The ultrastructure of chloroplasts was affected by water deficit and some starch grains (SG) appeared after one week of drought (D-1W). Moreover, after 2 weeks of water deficit (D-2W) grana lamellae (GL) loosened with severely swollen thylakoids and we noted the presence of enlarged SG. However, after 2 weeks of re-watering no apparent change on chloroplast structure was observed in both drought recovery regimes (Rec-D1 and Rec-D2) if compared to control samples usually (Fig. 4B).

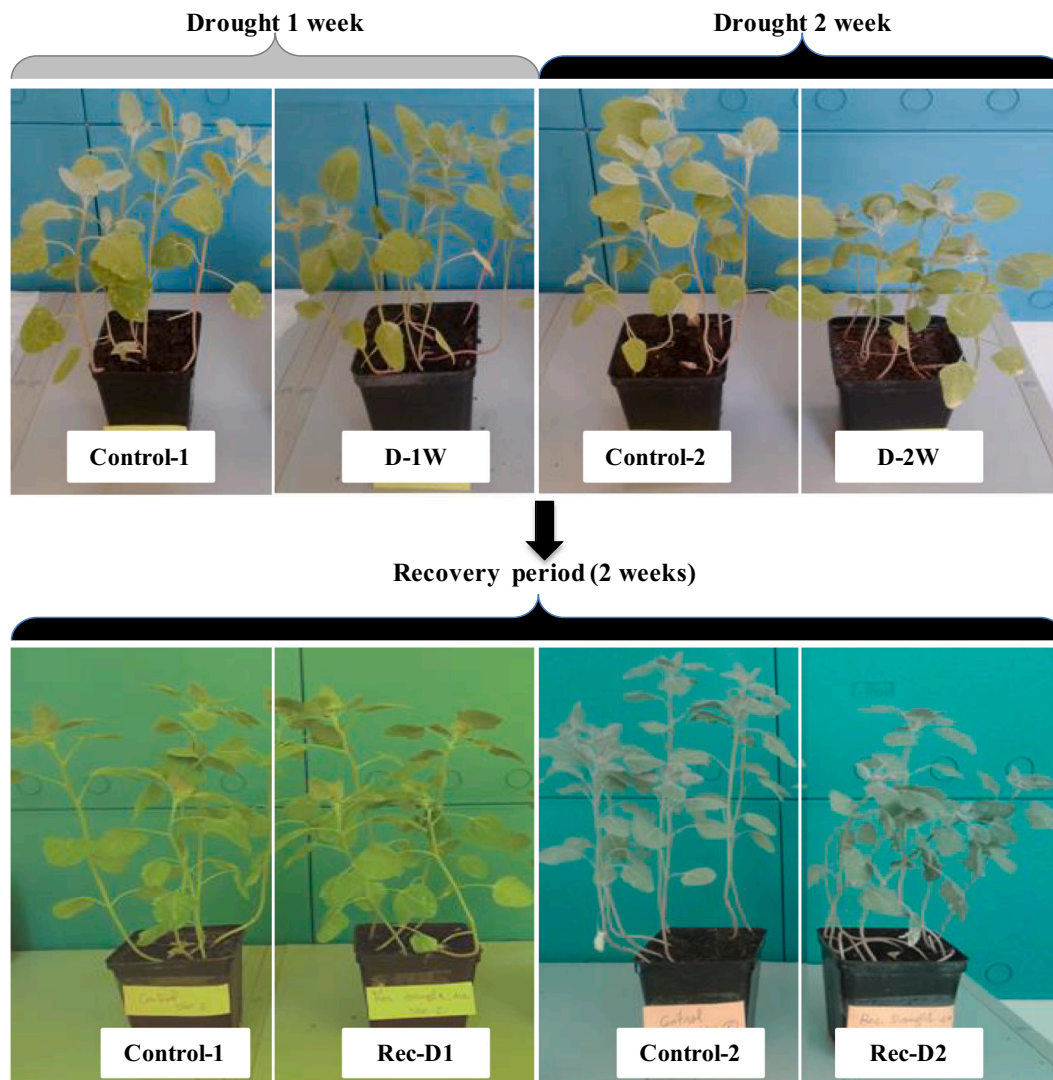


Fig. 2. Morphological aspects of quinoa plants cultivated under drought stress for one week (D-1W) or two weeks (D-2W). Each drought treatment was followed by a recovery period for two weeks (Rec-D1 and Rec-D2). Plant culture was conducted using a hydroponic system.

### 3.4. *Chl a* fluorescence induction (OJIP-curves) measurements

Recording the *Chl a* fluorescence induction (FI) on dark-adapted leaf for either control or drought-treated quinoa plant, showed some modifications in the obtained typical OJIP-curves (Fig. 5A). Drought treatment for one week (D-1W) induced an increase in the  $F_0$  value if compared to the control. This increase was more pronounced after 2 weeks of water deficit (D-2W). Furthermore, a decrease in  $F_m$  was noticed following drought stress application, especially for plants endured the stress for 2 weeks (D-2W). After the recovery period, no significant difference in  $F_m$  values was recorded between Ctrl and Rec-D1, while a small increase was detected with Rec-D2 treatment. It should be noted that water deficiency for 2 weeks (D-2W) entrained a considerable increase in the amplitude of  $F_v$  (variable fluorescence) at OJ and JI phases and a decrease in that of the IP phase as compared to Ctrl (Fig. 5A).

A normalization of the transient *Chl a* fluorescence ( $F_t/F_0$ ) was performed at  $F_0$  and showed a typical O, J, I and P steps (Fig. 5B). All applied water regimes showed a decrease in  $F_v$  of JI and IP phase as compared to the Ctrl, with a dramatic effect detected under (D-2W) treatment, where we observed a clear reduction of variable fluorescence at IP phase (Fig. 5B). Thus, the decrease in IP phase recorded after water

deficit (D-2W) was attenuated after the recovery period of 2 weeks (Rec-D2). In fact, after this recovery period, fluorescence rising based on Rec-D2 treatments, approximately reached the higher level than drought stressed plant (D-2W) but do not reached control level conditions (well-irrigated plants).

Drought treatment for one (D-1W) or two weeks (D-2W) induced an increase in the variable fluorescence  $V_{OJ}$  and  $V_{OK}$  as compared to the control (Fig. 5C and D). However, this increase was compensated after the recovery period where the (Rec-D1) and (Rec-D2) treatments approximately reached the control values especially for the variable fluorescence  $V_{OK}$  (Fig. 5C).

### 3.5. JIP-test parameters

Several biophysical parameters were derived from the transient fast *Chl a* FI (OJIP-curves) using Biolyzer v.3.0.6 software, which were (parameters) plotted in a spider chart (Fig. 6).  $S_M$  (the area above the OJIP-curve, represents the number of electrons that have to flow through the electron transport chain in order to reach  $F_m$ , [63]) remains constant during all drought treatments.

Considerable changes were observed in the energy and specific flux parameters regarding the water regimes compared to the control

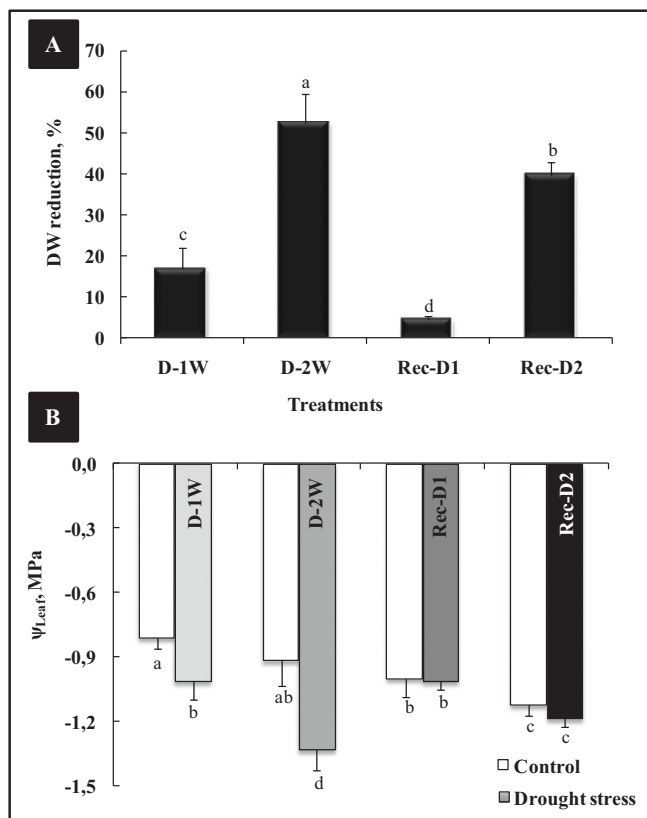


**Fig. 3.** Dry weight (DW) reduction (%) under drought stress compared to Ctrl (A) a leaf osmotic potential (B) of quinoa plants subjected to drought treatment for one (D-1W) or 2 weeks (D-2W) and after a recovery period for two weeks (Rec-D1 and Rec-D2) for each drought treatment. Data are means of 6 replicates  $\pm$  SE. Mean values with similar letters are not different at  $P$ -value  $< 0.05$  according to Duncan's multiple range test at 95%.

**Table 2**

Chlorophyll content in *Chenopodium quinoa* leaf submitted to different treatments (Ctrl, D-1W, D-2W, Rec-D1 and Rec-D2). Data are means of 6 replicates  $\pm$  SE. Means with similar letters are not different at  $P < 0.05$  according to Duncan's multiple range test at 95%.

	Chl a	Chl b	Tot Chl	Chl a/b ratio
Ctrl	0.858 $\pm$ 0.05 <sup>a</sup>	0.341 $\pm$ 0.02 <sup>a</sup>	1.19 $\pm$ 0.06 <sup>a</sup>	2.51 $\pm$ 0.09 <sup>a</sup>
D-1W	0.759 $\pm$ 0.06 <sup>ab</sup>	0.353 $\pm$ 0.01 <sup>a</sup>	1.11 $\pm$ 0.04 <sup>a</sup>	2.15 $\pm$ 0.10 <sup>b</sup>
D-2W	0.585 $\pm$ 0.04 <sup>c</sup>	0.231 $\pm$ 0.03 <sup>b</sup>	0.82 $\pm$ 0.04 <sup>c</sup>	2.53 $\pm$ 0.05 <sup>a</sup>
Rec-D1	0.694 $\pm$ 0.05 <sup>b</sup>	0.317 $\pm$ 0.04 <sup>a</sup>	1.01 $\pm$ 0.03 <sup>ab</sup>	2.18 $\pm$ 0.16 <sup>b</sup>
Rec-D2	0.691 $\pm$ 0.04 <sup>b</sup>	0.258 $\pm$ 0.02 <sup>b</sup>	0.95 $\pm$ 0.03 <sup>b</sup>	2.67 $\pm$ 0.17 <sup>a</sup>

(Fig. 6). Hence, drought stress induced an increase in ABS/RC and  $TR_0$ /RC. This increase was more obvious in  $DI_0$ /RC parameter after the D-2W treatment. However, these parameters were found to be lower under water recovery regimes (Rec-D1 and Rec-D2) than under drought treatment. In contrast,  $ET_0$ /RC decreased only after 2 weeks of drought (D-2W) relative to Ctrl, while it remains stable for the other treatments.

No significant change was noticed concerning the flux ratios parameter  $\phi_{P_0}$ , (maximum photochemical quantum yield) at all treatments, while a decrease in  $\psi_0$  and  $\phi_{E_0}$  was detected in drought stressed leaves particularly after 2 weeks (D-2W). After the recovery period, (Rec-D1) and (Rec-D2) treatments exhibited values of  $\psi_0$  and  $\phi_{E_0}$  similar to those observed for the control without drought (spider chart of Fig. 6).

The performance index  $PI_{(ABS)}$  showed a considerable decrease under water deficit regardless the drought stress duration (Fig. 6).  $PI_{ABS}$  was significantly reduced by about 26% after just 1 week of drought stress

(D-1W), if compared to the Ctrl. This decrease becomes more obvious and drastic after 2 weeks (D-2W) and reached about 70%. After the recovery period, the reduction in  $PI_{(ABS)}$  was about 40% and 22% under (Rec-D1) and (Rec-D2), respectively.

### 3.6. Energy conversion and electron transport rate through both photosystems (PSII and PSI)

Efficiency of energy conversion and electron transport rate through PSI and PSII in quinoa leaf were evaluated simultaneously using a Dual-PAM-100 system (Figs. 7–8). Both photosystems were influenced by water regimes but to various extents depending on the stress duration. In fact, a significant decrease in both quantum yields of PSI and PSII  $Y(I)$  and  $Y(II)$  was observed in drought-treated plants if compared to the control, particularly after 2 weeks of stress, D-2W (Fig. 7A, D). Conversely, with the recovery regimes (Rec-D1 and Rec-D2) the decrease in  $Y(I)$  was alleviated and no significant change was detected concerning  $Y(II)$  if compared to the other treatments.

Under drought stress conditions (D-1W and D-2W), the decrease in quantum yields  $Y(I)$  and  $Y(II)$  was accompanied, consecutively, by: (i) an increase of  $Y(ND)$  (quantum yield of non-photochemical energy dissipation in reaction centers due to PSI donor side limitation) (Fig. 7B) and (ii) an increase of  $Y(NPQ)$  (quantum yield of light-induced non-photochemical fluorescence quenching) (Fig. 7E). This effect (increase of  $Y(ND)$  and  $Y(NPQ)$ ) was more pronounced after 2 weeks of water deficit (D-2W); and was attenuated after the recovery period. In addition, a slight decrease in the  $Y(NA)$  (quantum yield of non-photochemical energy dissipation of RCs due to PSI acceptor side limitation) was observed in drought-stressed plants for both 1 (D-1W) and 2 weeks (D-2W) as compared to Ctrl (Fig. 7C). A restoration of this parameter ( $Y(NA)$ ) to a level similar to that of control plants was observed for both recovery periods (Rec-D1 and Rec-D2). At variance,  $Y(NO)$  (quantum yield of non-light-induced non-photochemical fluorescence quenching) remained unchanged among treatments except a small decrease under drought stress for 2 weeks, D-2W (Fig. 7F).

The electron transport rate through PSI (ETRI) decreased considerably under drought stress as compared to the control, with a drastic effect observed after 2 weeks of water deficit (Fig. 8A). After the recovery treatment, the decrease in ETRI was attenuated during both recovery periods (Rec-D1 and Rec-D2) but control levels remain usually not reached. No significant difference in the electron transport rate through PSII (ETRII) was observed after 1 week of drought (D-1W) or after the corresponding recovery period (Rec-D1) compared to Ctrl (Fig. 8B). In contrast, after 2 weeks of drought (D-2W) a decrease in ETRII was detected and it reached the control values after the termination of the recovery period (Rec-D2).

### 3.7. Amount of PSII proteins

The abundances of the main PSII proteins such as PsbA (D1), PsbB (CP47), PsbD (D2), PsbQ (P16), PsbO (OEC33) and LHCII, were semi-quantitatively evaluated by immunoblot (Fig. 9). Interesting changes affected PSII proteins in drought-treated plants, with very important differential responses depending on the stress duration and the recovery period. Indeed, the amount of protein D1 decreased significantly under water deficit for 1 week (D-1W) if compared to the Ctrl. Thus, this decrease was more accentuated and sharp after 2 weeks (D-2W). Moreover, the amount of D2, CP47, OEC and PsbQ proteins decreased significantly in drought-stressed plants with the same manner after 1 or 2 weeks of stress. After the recovery period, the damage to D1 protein detected in drought-treated plants was restored and reached the control levels. This explains the phenomenon of PSII proteins repair during the recovery process. Furthermore, the decrease in D2 protein amount was attenuated following the recovery regimes (Rec-D1 and Rec-D2) but its abundance remains still lower than in the control.

It is worthy that the decrease in the amount of CP47, OEC and PsbQ

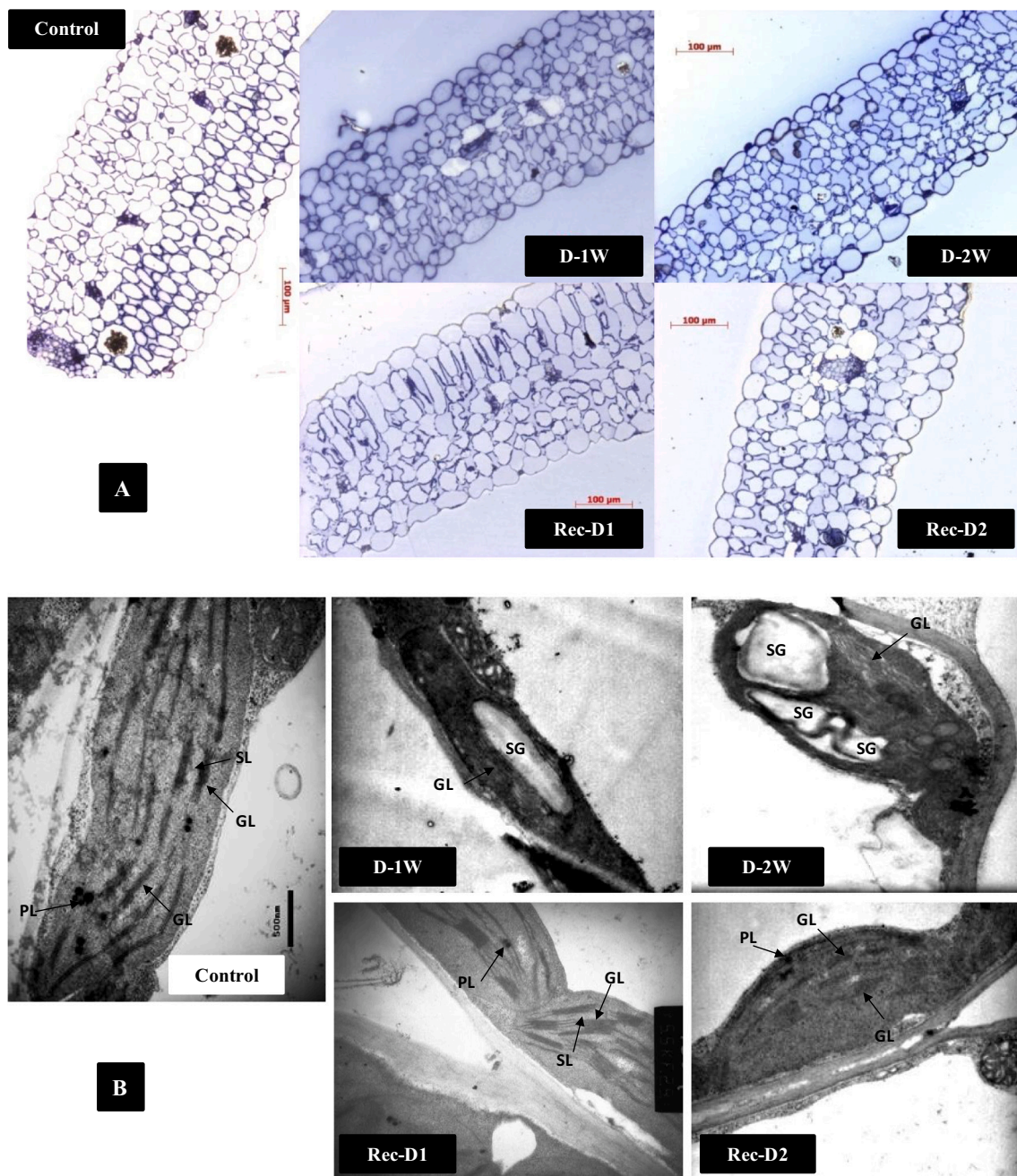


**Fig. 4.** Micrographs of leaf mesophyll cells obtained by light microscopy (A) and the ultrastructure of chloroplasts (B) obtained using transmission electron microscopy (TEM) for quinoa plants grown under either control or drought-treated for one (D-1W) or 2 weeks (D-2W) and following a recovery period of two weeks (Rec-D1 and Rec-D2) for each drought stress treatment. Ch: chloroplast, V: vacuole, GL: grana lamellae, SL: stroma lamellae, PL: plastoglobule, SG: starch grain.

protein complexes under drought stress (D-1W and D-2W) was compensated during the recovery period and even their proteins levels became higher under Rec-D1 and Rec-D2 treatments compared to the control before drought. This differential response of different PSII protein complexes to drought could be explained by the damage to some PSII proteins during drought and the ability of the PSII in quinoa to repair the damaged proteins during the recovery process and regain the full PSII activity and even better than before stress period for some proteins but not for other. The abundance of LHCII protein decreased significantly at all treatments in the same trend, except drought stress for 1 one week (D-1W) which showed no change if compared to control (Fig. 9).

#### 4. Discussion

This report reveals the performance of quinoa (*Chenopodium quinoa* Willd.) plants under drought stress. Notably, our results show a decrease in the plant growth and development under drought stress and the depressive effect of water deficit was more pronounced during the prolonged stress period (2 weeks). Similar results were observed in the xero-halophytic shrub *Atriplex halimus*, showing that the decrease in the growth rate was accompanied by a restriction in the leaf expansion, in response to a prolonged water deficit [64]. A decrease in the dry matter was also detected in the halophyte *Sesuvium portulacastrum* subjected to a water deficit of 25% FC [15] or following application of polyethylene glycol (PEG) or mannitol treatment [13]. In addition, water deficit induced a substantial decrease in the leaf expansion which was

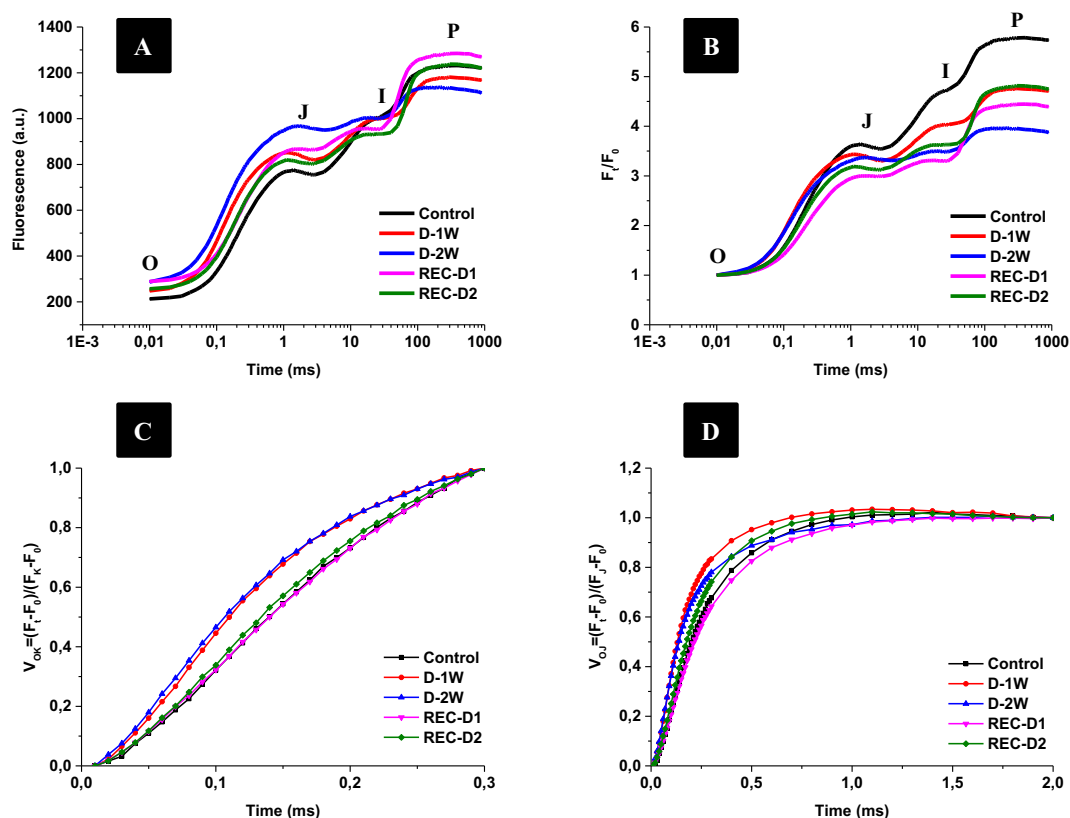


**Fig. 5.** Transient Chl *a* fluorescence (OJIP-curves) plotting at the logarithmic time scale for quinoa leaves obtained from plants grown under control or drought stress for either one (D-1W) or two weeks (D-2W) followed each by a recovery period for two weeks (Rec-D1 and Rec-D2). The OJIP curve showed the minimum fluorescence level  $F_0$  (O) and its maximum,  $F_m$  (P), with intermediate J- and I-steps. (A) Original Chl *a* fluorescence curves exhibit fluorescence intensity (a.u.; arbitrary unit). (B) Normalized data at  $F_0$  ( $F_t/F_0$ ). (C, D) Variable fluorescence  $V_{Ok}$  and  $V_{Oj}$  respectively, between control untreated and drought-treated plants either for one (D-1W) or two weeks (D-2W) followed by a recovery period for two weeks for each drought treatment (Rec-D1 and Rec-D2).

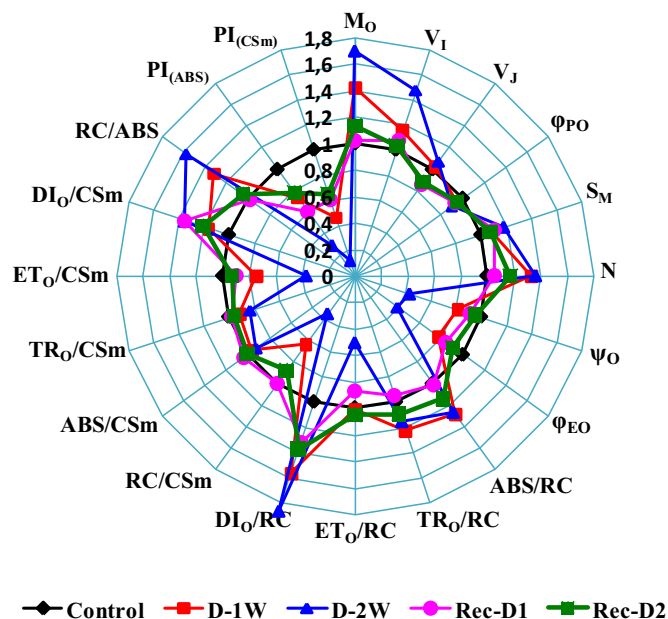


**Fig. 6.** A 'spider plot' of selected parameters derived from the Chl *a* fluorescence curve of untreated (Ctrl) or drought-treated plants for either one (D-1W) or two weeks (D-2W) followed by a recovery period for two weeks for each drought treatment (Rec-D1 and Rec-D2). All data of JIP-test parameters were normalized to the reference (Ctrl) and each variable at the reference was standardized by giving a numerical value of the unit (one).

concomitant to a considerable decline in the net photosynthesis assimilation (A) for two forage species *Sulla carnosa* and *Medicago truncatula* [45]. Overall, these clues suggested that the osmotic stress decreased the whole plant growth mainly through a restriction in the leaf expansion and plant photosynthesis. According to this investigation, water deficit led to a significant decrease in the leaf water potential during either short- or long-term drought stress. Upon recovery, this parameter was restored back to a level similar to that of control plants (Fig. 3B). This corroborates the ability of quinoa to cope with water stress and highlights its high capacity to maintain an appropriate tissue hydration and root development as previously demonstrated for two halophyte provenances of *Cakile maritima* exposed to a limiting water supply (mimicking 25% of FC) [65].

Several earlier reports have clearly emphasized that drought stress may directly affect photosynthesis through disrupting the cell organelles, by damaging the photosynthetic pigments, thylakoid membranes, chloroplasts ultra-structure and the photosynthetic electron transport chain, PETC [5,7,66,67]. Given that the chloroplasts constitute the primary target and that chloroplasts are most susceptible to various abiotic stresses [68,69], the prolonged drought stress period (D-2W) induced significant changes to the chloroplast organization, such as damage to envelope, losing of grana lamellae, severe swollen of thylakoids and presence of enlarged starch grains (SG, Fig. 4). Similar features have been reported under long-term drought period in maize [66], wheat [67] and *Leymus chinensis* [70]. However, an earlier study demonstrated that under severe drought the resistant cultivar of sugarcane (F172) maintained the integrity of its chloroplast structure [71].

Earlier observations revealed that the increased tolerance to drought and the recovery capacity could be tightly associated with the ability of preserving functional photochemical activity [72]. Our findings are in

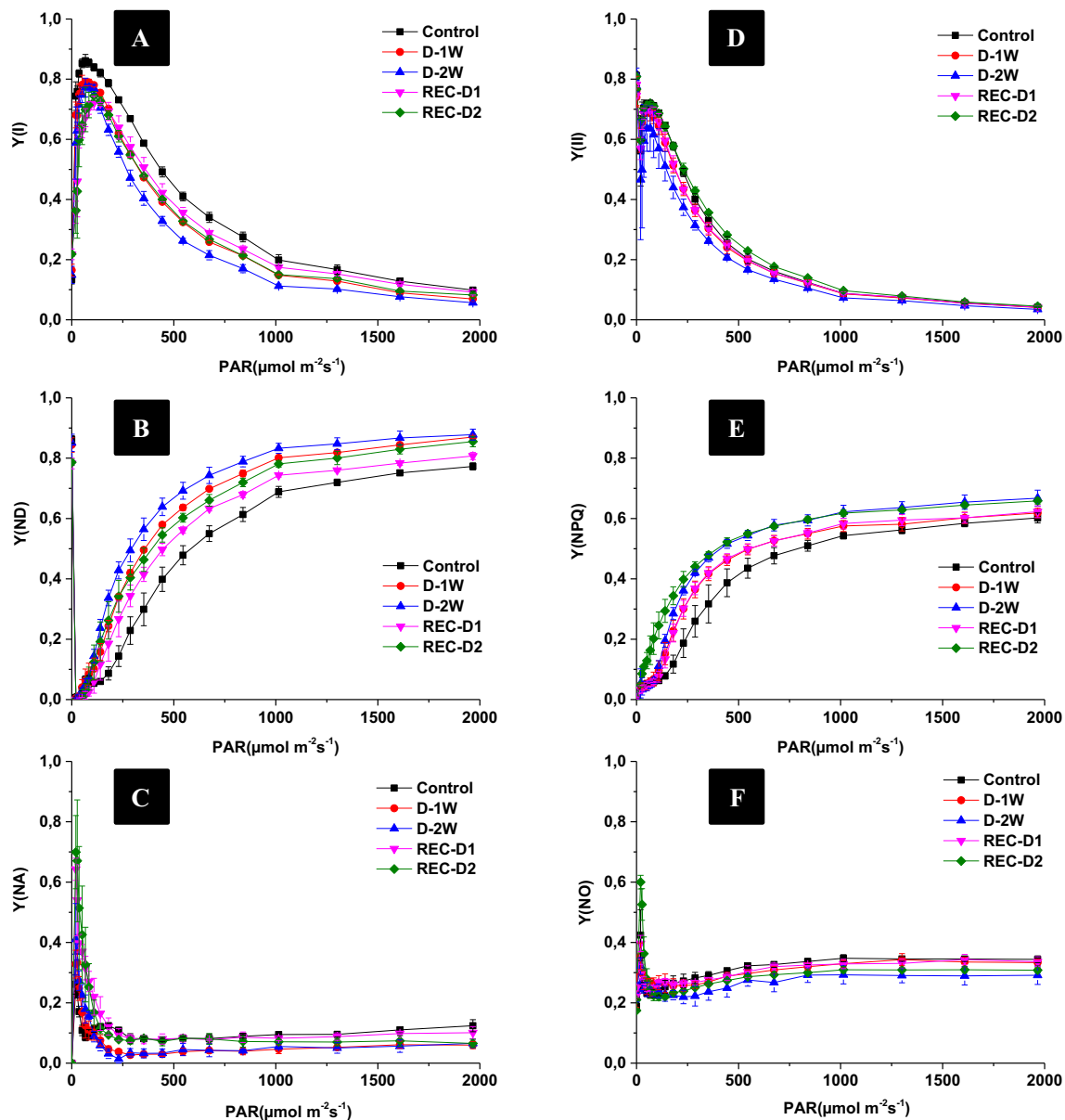


Fig. 7. (A, D) Photochemical quantum yield of PSI, Y(I), and PSII, Y(II). (B) Quantum yield of non-photochemical energy dissipation in PSII RCs, limited by donor side Y(ND). (C) Quantum yield of non-photochemical energy dissipation in reaction centers, limited by acceptor side Y(NA). (E) Quantum yield of light-induced non-photochemical fluorescence quenching Y(NPQ). (F) Quantum yield of non-light-induced non-photochemical fluorescence quenching Y(NO).

agreement with previous results conducted on two different species including  $C_3$  malacophyllous *Achillea ochroleuca* and CAM succulent *Sedum sexangulare*, where the obtained results showed broken thylakoid membrane systems, swollen grana, and SG accumulation; however, all these symptoms disappeared after re-watering [73]. In the current study, the observed accumulation of starch under long-term water deficit might be related to the loss of the photosynthetic activity, as previously emphasized [74]. This is also confirmed, especially by the loss of PSII core proteins (Fig. 9).

The biophysical approaches based on various techniques of Chl fluorescence (OJIP test and PAM analysis) were previously recognized as sensitive and powerful methods for the detection and assessment of plant response to stressful environmental conditions [25,50,75–78]. In fact, measurements of Chl *a* fluorescence kinetics deliver exhaustive information on the functional state of the photosynthetic apparatus, in particular PSII [40–42]. Thus, drought may directly or indirectly affect the kinetics and/or the shape of Chl *a* FI. Herein, we clearly showed that

drought induced some changes to the PSII primary photochemistry regarding the stress duration. Indeed, a prolonged water deficit induced an increase in  $F_0$  (Fig. 5A) which implies that the primary PSII acceptor,  $Q_A$ , was not fully oxidized and this could be attributed to the chlororespiration effect [79]. Hence, the  $F_0$  increase might be associated with the accumulation of  $Q_A^-$  in darkness as a redox poise with a partially reduced PQ pool, which could subsequently slow down the reduction of  $Q_A$ , the primary PSII quinone acceptor.

In this context, earlier study conducted on the perennial tree crop Mulberry (*Morus* spp.) grown under water deficit, demonstrated an elevation in  $F_0$  which could be attributed to a partially reduced PQ pool [80]. Besides, the gradual decrease in  $F_m$  during the stepwise drought reflects that the prolonged drought could be responsible for the thermal phase which induced a decrease in Chl *a* fluorescence at the IP phase and a reduction in the PSII electron transport [81]. It was earlier reported that following photodamage to OEC, the potential for damage to the PSII RCs would increase due to a restriction in the electron donation from the

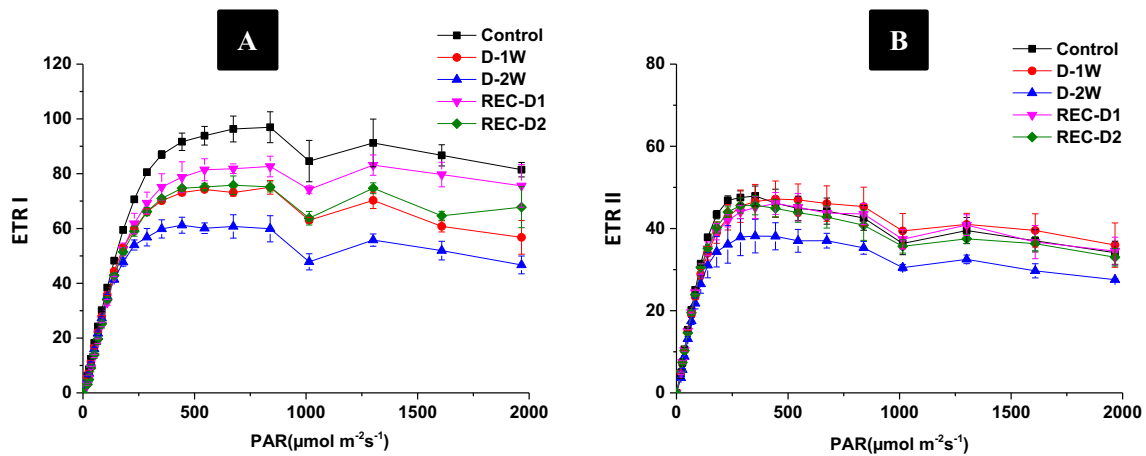


Fig. 8. Photosystems electron transport rates (ETR I and ETR II) measured on leaves of quinoa plants grown under control or drought stress for either one (D-1W) or 2 weeks (D-2W) followed by a recovery period for 2 weeks for each drought treatment (Rec-D1 and Rec-D2).

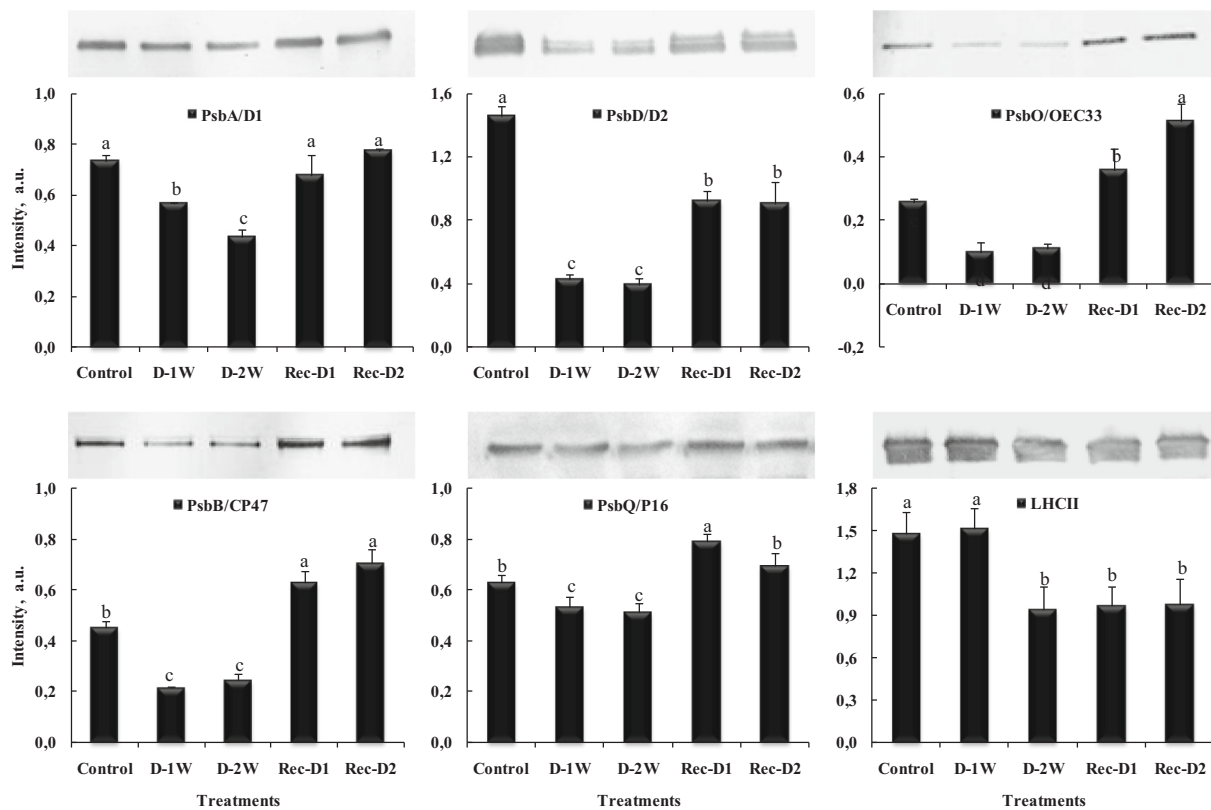


Fig. 9. Immunoblot analysis of thylakoid membrane proteins of untreated (Ctrl) and drought-treated plants for either one (D-1W) or 2 weeks (D-2W) then followed by a recovery period for 2 weeks for each drought treatment (Rec-D1 and Rec-D2). Each gel lane was loaded with 4 μg of proteins. Immunoblot analyses were performed using antibodies specific for PSII: D1, D2, CP47, LHCI, PsbQ and PsbO. Densitometric analysis of immunological reactions for antibodies was quantified using an *ImageJ* software. The histogram bars represent the averaged value (a.u. stands for arbitrary unit) calculated from three independent blots. Different alphabetic letters display the significant difference between treatments at  $P < 0.05$ .

OEC to the oxidized PSII RCs [82]. To cope with excessive light, stressed-plants have developed an adaptive mechanism to dissipate safely the excess of absorbed energy as heat [82]. Thus, our experiments agree with this strategy as reflected by the increase in  $DI_0/RC$  [50,83].

Drought stressed-plants were able to avoid PSII core complex damage where the decrease in the amount of D1, D2 and CP47 proteins was readjusted and recovered after rehydration (Fig. 9). In agreement with our results, a long-term drought-induced reduction in water content has led to a considerable depletion in the PSII of *Pisum sativum* [84]. The

remaining PSII complex appeared to be functionally reorganized with a unit size (LHCP/PSII core) two fold greater than that of well-irrigated plants and enhanced degradation of CP43 and D1 proteins. This remaining functional “surviving” PSII core was also demonstrated in our current investigation showing that the prolonged drought impaired the active PSII RCs but the inactivation process was not due to a physical destruction of the PSII core [85]. In addition, a relative stability in ETRII under drought could be accompanied by a decrease in the PSII proteins expression (such as D2 and CP47) which signifies that the electron

transport chain remains still intact and normally functional. Such observations suggested a kind of acclimation process for this halophyte thanks to the stability of chloroplast integrity under stress conditions [25].

To gain more insight about the impact of drought stress on PSII, we performed as well the JIP-test analysis using radar plot for the derived parameters from OJIP-curves (Fig. 6). Notably, it has been confirmed that drought stress causes some variations in energy absorption, energy and/or electron trapping, electron transport, and energy dissipation per cross section, which results in a reduction in the PSII efficiency [86,87]. Accordingly, some other studies have demonstrated that the increase in the ABS/RC under drought stress could be attributed to the decrease in the active RCs, i.e., which is probably associated to the double reduction of  $Q_A$  [80,88]. Consistently, our results show an increase in the ABS/RC and  $DI_0$ /RC ratios under drought stress, which was concurrent with a stable  $\phi_{P_0}$  (reflects the PSII primary photochemistry). The increase in ABS/RC might prevent the decrease in the electron transport rate (ETR), particularly under drought and ultimately favor the excess energy dissipation in order to reduce photodamage to the thylakoid system.

Our results of energy conversion and quantum yields showed a decrease in Y(I) and Y(II) and an increase in Y(ND) and Y(NPQ) under prolonged drought stress (Fig. 7), such observation tend towards to an appropriate photosynthetic control. This mechanism takes place during the occurrence of stomata closure, resulting thereby in the accumulation of reductant power (NADPH) and in a reduced ATP consumption, leading eventually to less organic matter and low plant yield. Under this so called “photosynthetic control” process, less electron flow through PSI would happen, contributing to a huge thylakoid lumen acidification, which triggers the photoprotective quenching mechanisms to dissipate safely the excess energy [89].

The photosynthesis efficiency in quinoa could be evaluated by determining the performance index  $PI_{(ABS)}$  which constitutes a very sensitive parameter to most of the abiotic stresses [53,60,90,91]. This integrative parameter estimates three main functional steps in PSII, i.e., the density of fully active RCs per absorption, the trapping of excitation energy and its conversion into the electron transport steps [92]. Thus, our results show a significant decrease in the  $PI_{(ABS)}$ , especially after long-term drought stress (D-2W) which suggests potentially a decrease in the PSII turnover and the level of electron transport through the PQ pool towards the oxidized P700 ( $P700^+$ ). Hence, similar results were previously reported and demonstrated a positive correlation between the  $CO_2$  assimilation rate and the  $PI_{(ABS)}$  values under drought [93].

## 5. Conclusion

The photosynthetic performance of quinoa submitted to gradual drought stress and recovery process was evaluated in the present study based on various Chl fluorescence techniques, chloroplast ultrastructure and immuno-blot analysis for the main PSII proteins. Our findings prompted us to deduce: 1) The structural integrity loss and the chloroplast arrangement disturbance could recover rapidly upon re-watering for both drought periods. 2) A prolonged drought could be responsible for the damping (or fall) of OEC capacity due to impairment of electron transport at the PSII donor side. 3) The electron transport chain remains active under different drought regimes. 4) The quinoa PSII supports well severe stressful conditions, including drought, and possesses a great potential and/or capacity to repair the damaged PSII protein complexes following stress. The flexibility of quinoa photosynthetic apparatus to drought seems strengthened thanks to the capacity of its efficient and robust physiological, biochemical and anatomical mechanisms to deal with the prevailing severe environmental conditions in its new climate of North Africa if compared to that of South America (original climate).

## Declaration of competing interest

The authors declare that they have no known competing financial

interests or personal relationships that could have appeared to influence the work reported in this paper.

## Acknowledgements

The authors acknowledge the Ministry of Higher Education and Scientific Research of Tunisia for financial support. Many thanks also to the United States Department of Agriculture (USDA) for providing quinoa seeds.

## References

- [1] D.W. Lawlor, Limitation to photosynthesis in water stressed leaves: stomata vs. metabolism and the role of ATP, *Ann. Bot.* 89 (2002) 871–885.
- [2] W. Wang, B. Vinocur, A. Altman, Plant responses to drought, salinity and extreme temperatures: towards genetic engineering for stress tolerance, *Planta* 218 (2003) 1–14.
- [3] A.R. Reddy, K.V. Chaitanya, M. Vivekanandan, Drought-induced responses of photosynthesis and antioxidant metabolism in higher plants, *J. Plant Physiol.* 161 (2004) 1189–1202.
- [4] G. Cornic, Drought stress and high light effects on leaf photosynthesis, in: N. R. Baker (Ed.), *Photoinhibition of photosynthesis: from molecular mechanisms to the field*. BIOS, Oxford, 1994, pp. 297–313.
- [5] D.W. Lawlor, G. Cornic, Photosynthetic carbon assimilation and associated metabolism in relation to water deficits in higher plants, *Plant Cell Environ.* 25 (2002) 275–294.
- [6] C.H. Foyer, G. Noctor, Oxygen processing in photosynthesis: regulation and signalling, *New Phytol.* 146 (2000) 359–388.
- [7] M.M. Chaves, Effects of water deficits on carbon assimilation, *J. Exp. Bot.* 42 (1991) 1–16.
- [8] H. Nayyar, D. Gupta, Differential sensitivity of C3 and C4 plants to water deficit stress: association with oxidative stress and antioxidants, *Environ. Exp. Bot.* 58 (2006) 106–113.
- [9] G. Noctor, S. Veljovic-Jovanovic, S. Driscoll, L. Novitskaya, C.H. Foyer, Drought and oxidative load in the leaves of C3 plants: a predominant role for photorespiration? *Ann. Bot.* 89 (2002) 841–850.
- [10] B. Halliwell, Reactive species and antioxidants. Redox biology is a fundamental theme of aerobic life, *Plant Physiol.* 141 (2006) 312–322.
- [11] H.-B. Shao, L.-Y. Chu, C.A. Jaleel, C.-X. Zhao, Water-deficit stress-induced anatomical changes in higher plants, *C. R. Biol.* 331 (2008) 215–225.
- [12] H.-B. Shao, L.-Y. Chu, G. Wu, J.-H. Zhang, Z.-H. Lu, Y.-C. Hu, Changes of some anti-oxidative physiological indices under soil water deficits among 10 wheat (*Triticum aestivum* L.) genotypes at tillering stage, *Colloids Surf. B* 54 (2007) 143–149.
- [13] I. Slama, T. Ghnaya, D. Messedi, K. Hessini, N. Labidi, A. Savoure, C. Abdely, Effect of sodium chloride on the response of the halophyte species *Sesuvium portulacastrum* grown in mannitol-induced water stress, *J. Plant Res.* 120 (2007) 291–299.
- [14] N. Youfi, I. Slama, T. Ghnaya, A. Savouré, C. Abdely, Effects of water deficit stress on growth, water relations and osmolyte accumulation in *Medicago truncatula* and *M. laciniata* populations, *C. R. Biol.* 333 (2010) 205–213.
- [15] I. Slama, D. Messedi, T. Ghnaya, A. Savoure, C. Abdely, Effects of water deficit on growth and proline metabolism in *Sesuvium portulacastrum*, *Environ. Exp. Bot.* 56 (2006) 231–238.
- [16] M. Ashraf, M.R. Foolad, Roles of glycine betaine and proline in improving plant abiotic stress resistance, *Environ. Exp. Bot.* 59 (2007) 206–216.
- [17] M.M. Chaves, J. Miguel Costa, N.J. Madeira Saibo, Recent advances in photosynthesis under drought and salinity, in: I. Turkan (Ed.), *Advances in Botanical Research* vol. 57, Academic Press, 2011, pp. 49–104.
- [18] S. Wilkinson, W.J. Davies, ABA-based chemical signalling: the co-ordination of responses to stress in plants, *Plant Cell Environ.* 25 (2002) 195–210.
- [19] A. Yang, S.S. Akhtar, M. Amjad, S. Iqbal, S.-E. Jacobsen, Growth and physiological responses of quinoa to drought and temperature stress, *J. Agron. Crop Sci.* 202 (2016) 445–453.
- [20] D.E. Jarvis, Y.S. Ho, D.J. Lightfoot, S.M. Schmöckel, B. Li, T.J.A. Borm, H. Ohyanagi, K. Mineta, C.T. Michell, N. Saber, N.M. Kharbatia, R.R. Rupper, A. R. Sharp, N. Dally, B.A. Boughton, Y.H. Woo, G. Gao, E.G.W.M. Schijlen, X. Guo, A. A. Momin, S. Negrão, S. Al-Babili, C. Gehring, U. Roessner, C. Jung, K. Murphy, S. T. Arold, T. Gojobori, C.G.v.d. Linden, E.N. van Loo, E.N. Jellen, P.J. Maughan, M. Tester, The genome of *Chenopodium quinoa*, *Nature* 542 (2017) 307.
- [21] S.-E. Jacobsen, F. Liu, C.R. Jensen, Does root-sourced ABA play a role for regulation of stomata under drought in quinoa (*Chenopodium quinoa* Willd.), *Sci. Hortic.* 122 (2009) 281–287.
- [22] H.-W. Koyro, S.S. Eisa, Effect of salinity on composition, viability and germination of seeds of *Chenopodium quinoa* Willd., *Plant Soil* 302 (2008) 79–90.
- [23] D. Bazile, S.-E. Jacobsen, A. Verniau, The Global Expansion of Quinoa: Trends and Limits, *Frontiers in Plant Science*, 7, 2016.
- [24] W. Derbali, R. Goussi, H.-W. Koyro, C. Abdely, A. Manaa, Physiological and biochemical markers for screening salt tolerant quinoa genotypes at early seedling stage, *J. Plant Interact.* 15 (2020) 27–38.
- [25] A. Manaa, R. Goussi, W. Derbali, S. Cantamessa, C. Abdely, R. Barbato, Salinity tolerance of quinoa (*Chenopodium quinoa* Willd.) as assessed by chloroplast

- ultrastructure and photosynthetic performance, *Environ. Exp. Bot.* 162 (2019) 103–114.
- [26] S. Shabala, Y. Hariadi, S.-E. Jacobsen, Genotypic difference in salinity tolerance in quinoa is determined by differential control of xylem Na<sup>+</sup> loading and stomatal density, *J. Plant Physiol.* 170 (2013) 906–914.
- [27] F. Razzaghi, S.H. Ahmadi, V.I. Adolf, C.R. Jensen, S.-E. Jacobsen, M.N. Andersen, Water relations and transpiration of quinoa (*Chenopodium quinoa* Willd.) under salinity and soil drying, *J. Agron. Crop Sci.* 197 (2011) 348–360.
- [28] F. Razzaghi, S.H. Ahmadi, S.-E. Jacobsen, C.R. Jensen, M.N. Andersen, Effects of salinity and soil-drying on radiation use efficiency, water productivity and yield of quinoa (*Chenopodium quinoa* Willd.), *J. Agron. Crop Sci.* 198 (2012) 173–184.
- [29] F. Razzaghi, S.-E. Jacobsen, C.R. Jensen, M.N. Andersen, Ionic and photosynthetic homeostasis in quinoa challenged by salinity and drought – mechanisms of tolerance, *Funct. Plant Biol.* 42 (2015) 136–148.
- [30] S.E. Jacobsen, C. Monteros, J.L. Christiansen, L.A. Bravo, L.J. Corcuera, A. Mujica, Plant responses of quinoa (*Chenopodium quinoa* Willd.) to frost at various phenological stages, *Eur. J. Agron.* 22 (2005) 131–139.
- [31] S.E. Jacobsen, C. Monteros, L.J. Corcuera, L.A. Bravo, J.L. Christiansen, A. Mujica, Frost resistance mechanisms in quinoa (*Chenopodium quinoa* Willd.), *Eur. J. Agron.* 26 (2007) 471–475.
- [32] K.B. Ruiz, S. Biondi, E.A. Martínez, F. Orsini, F. Antognoni, S.E. Jacobsen, Quinoa – a model crop for understanding salt-tolerance mechanisms in halophytes, *Plant Biosyst.* 150 (2015) 357–371.
- [33] K.B. Ruiz, S. Biondi, R. Oses, I.S. Acuña-Rodríguez, F. Antognoni, E.A. Martínez-Mosqueira, A. Coulibaly, A. Canahua-Murillo, M. Pinto, A. Zurita-Silva, D. Bazile, S.-E. Jacobsen, M.A. Molina-Montenegro, Quinoa biodiversity and sustainability for food security under climate change. A review, *Agron. Sustain. Dev.* 34 (2014) 349–359.
- [34] D.D. Bazile, C. Pulvento, A. Verniau, M.S. Al-Nusairi, D. Ba, J. Breidy, L. Hassan, M. I. Mohammed, O. Mambetov, M. Otambekova, N.A. Sepahvand, A. Shams, D. Souici, K. Miri, S. Padulosi, Worldwide evaluations of quinoa: preliminary results from post international year of quinoa FAO projects in nine countries, *Front. Plant Sci.* 7 (2016) 850.
- [35] O. Benhabib, A. Yazar, M. Qadir, E. Lourenço, S.E. Jacobsen, How can we improve mediterranean cropping systems? *J. Agron. Crop Sci.* 200 (2014) 325–332.
- [36] V. Nowak, J. Du, U.R. Charrondière, Assessment of the nutritional composition of quinoa (*Chenopodium quinoa* Willd.), *Food Chem.* 193 (2016) 47–54.
- [37] R. Repo-Carrasco, C. Espinoza, S.E. Jacobsen, Nutritional value and use of the andean crops quinoa (*Chenopodium quinoa*) and Kañiwa (*Chenopodium pallidicaule*), *Food Rev. Int.* 19 (2003) 179–189.
- [38] A. Vega-Gálvez, M. Miranda, J. Vergara, E. Uribe, L. Puente, E.A. Martínez, Nutrition facts and functional potential of quinoa (*Chenopodium quinoa* willd.), an ancient Andean grain: a review, *J. Sci Food Agric.* 90 (2010) 2541–2547.
- [39] D. Bazile, F. Baudron, The dynamics of the global expansion of quinoa growing in view of its high biodiversity, in: D. Bazile, H.D. Bertero, C. Nieto (Eds.), State of the Art Report on Quinoa Around the World in 2013, FAO & CIRAD, Roma, 2015, pp. 42–55.
- [40] P. Dąbrowski, A.H. Baczewska-Dąbrowska, H.M. Kalaji, V. Goltsev, M. Paunov, M. Rapacz, M. Wójcik-Jagła, B. Pawluśkiewicz, W. Bąba, M. Brestic, Exploration of chlorophyll a fluorescence and plant gas exchange parameters as indicators of drought tolerance in perennial ryegrass, *Sensors* 19 (2019) 2736.
- [41] P. Faseela, A.K. Sinisha, M. Brestic, J.T. Puthur, Special issue in honour of Prof. Reto J. Strasser - chlorophyll a fluorescence parameters as indicators of a particular abiotic stress in rice, *Photosynthetica* 58 (2020) 293–300.
- [42] R. Fghire, F. Anaya, O.I. Ali, O. Benhabib, R. Ragab, S. Wahbi, Physiological and photosynthetic response of quinoa to drought stress, *Chilean Journal of Agricultural Research* 75 (2015) 174–183.
- [43] J.-R. Acosta-Motos, P. Diaz-Vivancos, S. Álvarez, N. Fernández-García, M. J. Sanchez-Blanco, J.A. Hernández, Physiological and biochemical mechanisms of the ornamental *Eugenia myrtifolia* L. plants for coping with NaCl stress and recovery, *Planta* 242 (2015) 829–846.
- [44] K. Parvin, M. Hasanuzzaman, M.H.M.B. Bhuyan, K. Nahar, S.M. Mohsin, M. Fujita, Comparative physiological and biochemical changes in tomato (*Solanum lycopersicum* L.) under salt stress and recovery: role of antioxidant defense and glyoxalase systems, *Antioxidants* 8 (2019) 350.
- [45] A. Rouached, I. Slama, W. Zorrig, A. Jdey, C. Cukier, M. Rabhi, O. Talbi, A. M. Limami, C. Abdely, Differential performance of two forage species, *Medicago truncatula* and *Sulla carnosa*, under water-deficit stress and recovery, *Crop and Pasture Science* 64 (2013) 254–264.
- [46] D.K. Cassel, D.R. Nielsen, Field capacity and available water capacity, in: A. Klute (Ed.), *Methods of Soil Analysis*, 2nd edn. Am. Soc. Agron. Monograph No. 9, 1986, pp. 901–926. Part 2.
- [47] E.J. Hewitt, Sand and water culture methods used in the study of plant nutrition. (Commonwealth Agricultural Bureaux: Farnham Royal, England), *Tech. Commun.*, 22, Commonwealth Agric. Bureau, Farnham Royal, 2nd edn, 1966, 547 pp.
- [48] A. Manaa, H. Mimouni, S. Wasti, E. Gharbi, S. Aschi-Smiti, M. Faurobert, H. B. Ahmed, Comparative proteomic analysis of tomato (*Solanum lycopersicum*) leaves under salinity stress, *Plant Omics* 6 (2013) 268–277.
- [49] H.H.K. Lichtenthaler, [34] Chlorophylls and carotenoids: Pigments of photosynthetic biomembranes, in: *Methods in Enzymology* vol. 148, Academic Press, 1987, pp. 350–382.
- [50] R. Goussi, A. Manaa, W. Derbali, S. Cantamessa, C. Abdely, R. Barbato, Comparative analysis of salt stress, duration and intensity, on the chloroplast ultrastructure and photosynthetic apparatus in *Thellungiella salsuginea*, *J. Photochem. Photobiol. B* 183 (2018) 275–287.
- [51] J.H. Luft, Improvements in epoxy resin embedding methods, *J. Biophys. Biochem. Cytol.* 9 (1961) 409–414.
- [52] E.S. Reynolds, The use of lead citrate at high pH as an electron-opaque stain in electron microscopy, *J. Cell Biol.* 17 (1963) 208–212.
- [53] R.J. Strasser, M. Tsimilli-Michael, S.A., Analysis of the fluorescence transient, in: C. George, C. Papageorgiou, Govindjee (Eds.), *Chlorophyll Fluorescence: A Signature of Photosynthesis*, Advances in Photosynthesis and Respiration Series, Springer, Dordrecht, 2004, pp. 321–362.
- [54] R.J. Strasser, A. Srivastava, Govindjee, Polyphasic chlorophyll a fluorescence transient in plants and cyanobacteria, *Photochem. Photobiol.* 61 (1995) 32–42.
- [55] A. Stirbet, Govindjee, on the relation between the Kautsky effect (chlorophyll a fluorescence induction) and photosystem II: basics and applications of the OJIP fluorescence transient, *J. Photochem. Photobiol. B* 104 (2011) 236–257.
- [56] R. Strasser, A. Srivastava, I.M. Tsimilli-Michael, The fluorescence transient as a tool to characterize and screen photosynthetic samples, in: P. Mohanty, Pathre Yunus (Eds.), *Probing Photosynthesis: Mechanism, Regulation and Adaptation*, Taylor and Francis, London, 2000, pp. 443–480.
- [57] C. Klughammer, U. Schreiber, Complementary PS II quantum yields calculated from simple fluorescence parameters measured by PAM fluorometry and the saturation pulse method, *PAM Application Notes* 1 (2008) 27–35.
- [58] C. Klughammer, U. Schreiber, Saturation pulse method for assessment of energy conversion in PS I, *Planta* 192 (1994) 261–268.
- [59] N.R. Baker, Chlorophyll fluorescence: a probe of photosynthesis in vivo, *Annu. Rev. Plant Biol.* 59 (2008) 89–113.
- [60] R. Goussi, A. Manaa, W. Derbali, T. Ghnaya, C. Abdely, R. Barbato, Combined effects of NaCl and Cd<sup>2+</sup> stress on the photosynthetic apparatus of *Thellungiella salsuginea*, *Biochim. Biophys. Acta* 1859 (2018) 1274–1287.
- [61] R. Barbato, G. Friso, F. Rigoni, F. Dalla Vecchia, G.M. Giacometti, Structural changes and lateral redistribution of photosystem II during donor side photoinhibition of thylakoids, *J. Cell Biol.* 119 (1992) 325–335.
- [62] D.I. Arnon, Copper enzymes in isolated chloroplasts. Polyphenoloxidase in *Beta vulgaris*, *Plant Physiol.* 24 (1949) 1–15.
- [63] S.Z. Tóth, G. Schansker, R.J. Strasser, A non-invasive assay of the plastoquinone pool redox state based on the OJIP-transient, *Photosynth. Res.* 93 (2007) 193.
- [64] J.-P. Martinez, S. Lutts, A. Schanck, M. Bajji, J.-M. Kinet, Is osmotic adjustment required for water stress resistance in the Mediterranean shrub *Atriplex halimus* L? *J. Plant Physiol.* 161 (2004) 1041–1051.
- [65] A. Jdey, I. Slama, A. Rouached, C. Abdely, Growth, Na<sup>+</sup>, K<sup>+</sup>, osmolyte accumulation and lipid membrane peroxidation of two provenances of *Cakile maritima* during water deficit stress and subsequent recovery, *Flora* 209 (2014) 54–62.
- [66] R.X. Shao, L.F. Xin, H.F. Zheng, L.L. Li, W.L. Ran, J. Mao, Q.H. Yang, Changes in chloroplast ultrastructure in leaves of drought-stressed maize inbred lines, *Photosynthetica* 54 (2016) 74–80.
- [67] V. Vassileva, K. Demirevska, L. Simova-Stoilova, T. Petrova, N. Tsenov, U. Feller, Long-term field drought affects leaf protein pattern and chloroplast ultrastructure of winter wheat in a cultivar-specific manner, *J. Agron. Crop Sci.* 198 (2012) 104–117.
- [68] J. Molas, Changes of chloroplast ultrastructure and total chlorophyll concentration in cabbage leaves caused by excess of organic Ni(II) complexes, *Environ. Exp. Bot.* 47 (2002) 115–126.
- [69] L.D. Noodén, J.J. Guimét, J. I, 15–Whole plant senescence, in: L.D. Noodén (Ed.), *Plant Cell Death Processes*, Academic Press, San Diego, 2004, pp. 227–244.
- [70] Z.Z. Xu, G.S. Zhou, H. Shimizu, Effects of soil drought with nocturnal warming on leaf stomatal traits and mesophyll cell ultrastructure of a perennial grass, *Crop Sci.* 49 (2009) 1843–1851.
- [71] F.-J. Zhang, K.-K. Zhang, C.-Z. Du, J. Li, Y.-X. Xing, L.-T. Yang, Y.-R. Li, Effect of drought stress on anatomical structure and chloroplast ultrastructure in leaves of sugarcane, *Sugar Tech* 17 (2015) 41–48.
- [72] A. Trotta, S. Redondo-Gómez, C. Pagliano, M.E.F. Clemente, N. Rascio, N. La Rocca, A. Antonacci, F. Andreucci, R. Barbato, Chloroplast ultrastructure and thylakoid polypeptide composition are affected by different salt concentrations in the halophytic plant *Arthrocnemum macrostachyum*, *J. Plant Physiol.* 169 (2012) 111–116.
- [73] I. Maróti, Z. Tuba, M. Csik, Changes of chloroplast ultrastructure and carbohydrate level in *Festuca*, *Achillea* and *Sedum* during drought and after recovery, *J. Plant Physiol.* 116 (1984) 1–10.
- [74] R.N. Mutava, S.J.K. Prince, N.H. Syed, L. Song, B. Valliyodan, W. Chen, H. T. Nguyen, Understanding abiotic stress tolerance mechanisms in soybean: a comparative evaluation of soybean response to drought and flooding stress, *Plant Physiol. Biochem.* 86 (2015) 109–120.
- [75] M. Brestic, M. Zivcak, PSII fluorescence techniques for measurement of drought and high temperature stress signal in crop plants: protocols and applications, in: G. R. Rout, A.B. Das (Eds.), *Molecular Stress Physiology of Plants*, Springer India, India, 2013, pp. 87–131.
- [76] J. Essemine, S. Govindachary, S. Ammar, S. Bouzid, R. Carpentier, Enhanced sensitivity of the photosynthetic apparatus to heat stress in digalactosyl-diacylglycerol deficient *Arabidopsis*, *Environ. Exp. Bot.* 80 (2012) 16–26.
- [77] J. Essemine, Y. Xiao, M. Qu, H. Mi, X.-G. Zhu, Cyclic electron flow may provide some protection against PSII photoinhibition in rice (*Oryza sativa* L.) leaves under heat stress, *J. Plant Physiol.* 211 (2017) 138–146.
- [78] H.M. Kalaji, L. Račková, V. Paganová, T. Swoczyna, S. Rusinowski, K. Sitko, Can chlorophyll-a fluorescence parameters be used as bio-indicators to distinguish between drought and salinity stress in *Tilia cordata* Mill? *Environ. Exp. Bot.* 152 (2018) 149–157.

- [79] L.A. Sazanov, P.A. Burrows, P.J. Nixon, The plastid *ndh* genes code for an NADH-specific dehydrogenase: isolation of a complex I analogue from pea thylakoid membranes, *Proc. Natl. Acad. Sci.* 95 (1998) 1319–1324.
- [80] A. Guha, D. Sengupta, A.R. Reddy, Polyphasic chlorophyll a fluorescence kinetics and leaf protein analyses to track dynamics of photosynthetic performance in mulberry during progressive drought, *Photochem. Photobiol.* 119 (2013) 71–83.
- [81] A. Srivastava, B. Guissé, H. Greppin, R.J. Strasser, Regulation of antenna structure and electron transport in photosystem II of *Pisum sativum* under elevated temperature probed by the fast polyphasic chlorophyll a fluorescence transient: OKJIP, *Biochimica et Biophysica Acta (BBA) - Bioenergetics* 1320 (1997) 95–106.
- [82] S. Takahashi, M.R. Badger, Photoprotection in plants: a new light on photosystem II damage, *Trends Plant Sci.* 16 (2011) 53–60.
- [83] A.R. Falqueto, R.A. da Silva Júnior, M.T.G. Gomes, J.P.R. Martins, D.M. Silva, F. L. Partelli, Effects of drought stress on chlorophyll a fluorescence in two rubber tree clones, *Sci. Hortic.* 224 (2017) 238–243.
- [84] M.T. Giardi, A. Cona, B. Geiken, T. Kučera, J. Masojídek, A.K. Mattoo, Long-term drought stress induces structural and functional reorganization of photosystem II, *Planta* 199 (1996) 118–125.
- [85] E.M. Aro, I. Virgin, B. Andersson, Photoinhibition of Photosystem II. Inactivation, protein damage and turnover, *Biochim. Biophys. Acta.* 1143 (1993) 113–134.
- [86] K. Khatri, M.S. Rathore, Photosystem photochemistry, prompt and delayed fluorescence, photosynthetic responses and electron flow in tobacco under drought and salt stress, *Photosynthetica* 57 (2019) 61–74.
- [87] A. Střibet, D. Lázár, J. Kromdijk, Govindjee, Chlorophyll a fluorescence induction: can just a one-second measurement be used to quantify abiotic stress responses? *Photosynthetica* 56 (2018) 86–104.
- [88] R.J. Strasser, A.D. Střibet, Heterogeneity of photosystem II probed by the numerically simulated chlorophyll a fluorescence rise (O–J–I–P), *Math. Comput. Simul.* 48 (1998) 3–9.
- [89] V. Nagy, A. Podmaniczki, A. Vidal-Meireles, R. Tengölics, L. Kovács, G. Rákhely, A. Scoma, S.Z. Tóth, Water-splitting-based, sustainable and efficient H<sub>2</sub> production in green algae as achieved by substrate limitation of the Calvin–Benson–Bassham cycle, *Biotechnology for Biofuels* 11 (2018) 69.
- [90] A. Oukarroum, S.E. Madidi, G. Schansker, R.J. Strasser, Probing the responses of barley cultivars (*Hordeum vulgare* L.) by chlorophyll a fluorescence OLKJIP under drought stress and re-watering, *Environ. Exp. Bot.* 60 (2007) 438–446.
- [91] M. Živcak, M. Brestic, K. Olsovska .S.P., Performance index as a sensitive indicator of water stress in *Triticum aestivum* L, *Plant Soil Environ.* 54 (2008) 133–139.
- [92] H.M. Kalaji, K. Govindjee, J. Bosa, K. Kościelniak, Żuk-Gotaszewska, Effects of salt stress on photosystem II efficiency and CO<sub>2</sub> assimilation of two Syrian barley landraces, *Environ. Exp. Bot.* 73 (2011) 64–72.
- [93] P.D.R. van Heerden, J.W. Swanepoel, G.H.J. Krüger, Modulation of photosynthesis by drought in two desert scrub species exhibiting C3-mode CO<sub>2</sub> assimilation, *Environ. Exp. Bot.* 61 (2007) 124–136.